Since January 2020 Elsevier has created a COVID-19 resource centre with free information in English and Mandarin on the novel coronavirus COVID-19. The COVID-19 resource centre is hosted on Elsevier Connect, the company's public news and information website.

Antiviral Research 120 (2015) 101–111

Contents lists available at ScienceDirect

Antiviral Research

journal homepage: www.elsevier.com/locate/antiviral

Mouse lung slices: An *ex vivo* model for the evaluation of antiviral and anti-inflammatory agents against influenza viruses

Rui Liu [a,b], Liwei An [a,b,c], Ge Liu [a,b], Xiaoyu Li [a,b], Wei Tang [a], Xulin Chen [a,b,*]

[a] State Key Laboratory of Virology, Wuhan Institute of Virology, Chinese Academy of Sciences, Wuhan 43001, Hubei, China
[b] University of Chinese Academy of Sciences, Beijing 100049, China
[c] Department of Anatomy, The University of Hong Kong, Hong Kong, China[1]

ARTICLE INFO

Article history:
Received 31 January 2015
Revised 21 May 2015
Accepted 25 May 2015
Available online 27 May 2015

Keywords:
Lung slice
Influenza virus
Cytokine
Chemokine
Antiviral
Anti-inflammatory

ABSTRACT

The influenza A virus is notoriously known for its ability to cause recurrent epidemics and global pandemics. Antiviral therapy is effective when treatment is initiated within 48 h of symptom onset, and delaying treatment beyond this time frame is associated with decreased efficacy. Research on anti-inflammatory therapy to ameliorate influenza-induced inflammation is currently underway and seems important to the impact on the clinical outcome. Both antiviral and anti-inflammatory drugs with novel mechanisms of action are urgently needed. Current methods for evaluating the efficacy of anti-influenza drugs rely mostly on transformed cells and animals. Transformed cell models are distantly related to physiological and pathological conditions. Although animals are the best choices for preclinical drug testing, they are not time- or cost-efficient. In this study, we established an *ex vivo* model using mouse lung slices to evaluate both antiviral and anti-inflammatory agents against influenza virus infection. Both influenza virus PR8 (H1N1) and A/Human/Hubei/3/2005 (H3N2) can replicate efficiently in mouse lung slices and trigger significant cytokine and chemokine responses. The induction of selected cytokines and chemokines were found to have a positive correlation between *ex vivo* and *in vivo* experiments, suggesting that the *ex vivo* cultured lung slices may closely resemble the lung functionally in an *in vivo* configuration when challenged by influenza virus. Furthermore, a set of agents with known antiviral and/or anti-inflammatory activities were tested to validate the *ex vivo* model. Our results suggested that mouse lung slices provide a robust, convenient and cost-efficient model for the assessment of both antiviral and anti-inflammatory agents against influenza virus infection in one assay. This *ex vivo* model may predict the efficacy of drug candidates' antiviral and anti-inflammatory activities *in vivo*.

1. Introduction

Influenza A virus (IAV) is still a threat to human health and poses a global concern due to its unpredictable, pandemic potential and pathogenesis. As high evolutionary rates of the influenza virus makes vaccination strategies difficult, anti-influenza drugs are crucial for the control of influenza pandemics. Antiviral therapy is generally licensed for use within 48 h of influenza illness onset, and delaying treatment is associated with decreased drug efficacy and increased morbidity and mortality (Kandun et al., 2008). Although influenza-induced pathology is still unclear, the uncontrolled immune response may be the major contributor to influenza virus-induced mortality (de Jong et al., 2006; Iwasaki and Medzhitov, 2011; Kobasa et al., 2007). Thus, studies on the modulation of the host immune response are currently underway. Several animal studies have shown that anti-inflammatory agents

Abbreviations: TNF-α, tumour necrosis factor alpha; IL-6, interleukin 6; RANTES, regulated on activation, normal T cell expressed and secreted; MIP-3α, macrophage inflammatory protein 3 alpha; IP-10, interferon-gamma induced protein 10; IL-10, interleukin 10; IL-1β, interleukin 1 beta; IFN-γ, interferon gamma; PPAR-γ, peroxisome proliferator-activated receptor gamma; EGCG, epigallocatechin gallate; CXCR3, chemokine (C-X-C motif) receptor 3; TNFR1, tumour necrosis factor alpha receptor 1; IL-1R, interleukin 1 receptor; MIP-1, macrophage inflammatory protein 1; CCR2, C-C chemokine receptor type 2; GM-CSF, Granulocyte–macrophage colony-stimulating factor; i.p., intraperitoneal; BALF, bronchoalveolar lavage fluid; RIG-I, retinoic acid-inducible gene I; TLR 7/8, toll-like receptor 7/8; TLR 3, toll-like receptor 3; MUNANA, 2′-(4-methylumbelliferyl)-α-D-acetylneuraminic acid.

* Corresponding author at: Wuhan Institute of Virology, Chinese Academy of Sciences, 44 Xiao Hong Shan Zhong Qu, Wuchang District, Wuhan, Hubei 430071, China.

E-mail address: chenxl@wh.iov.cn (X. Chen).

[1] Current address.

http://dx.doi.org/10.1016/j.antiviral.2015.05.008
0166-3542/

can protect mice from death against influenza infection. 15-deoxy-$\Delta^{12,14}$-prostaglandin J_2 (15d-PGJ_2) has been shown to protect 79% of mice from death against lethal influenza infection through manipulation of the PPAR-γ pathway, whereas it does not inhibit virus replication (Cloutier et al., 2012). The P38 inhibitor significantly protects mice from lethal influenza infection without affecting virus replication (Borgeling et al., 2014). Statins not only reduce the levels of LDL-cholesterol, but they also counteract the inflammatory changes associated with acute coronary syndrome and improve survival in patients with influenza. Similarly, in patients hospitalised with laboratory-confirmed seasonal influenza, statin treatment is associated with a 41% reduction in 30-day mortality (Fedson, 2013). Therefore, strategies targeting aberrant host immune responses may be good complements for existing antiviral drugs.

The routine strategies for anti-influenza drug development rely primarily on cell-based assays in primary screening followed by animal studies. However, the cost of *in vivo* studies is very high due to the use of animals and a large quantity of investigational compounds. Lung slices, which provide a bridge between single cells and whole animals, are broadly used in physiology and toxicity studies (Morin et al., 2013; Sanderson, 2011). Different from single cell lines, lung slices possess multiple cell types and preserve the physiological and functional cellular relationships within the body. Cell–cell and cell–matrix interactions result in lung slices closely resembling the morphology and functionality of the lung. Whereas the evaluation of the efficacy of a drug based on animal studies is expensive and time-consuming, the lung slice model may serve as a valuable tool for efficacy tests of compounds for the treatment of influenza. With the development of tissue slicers, which produce slices rapidly and reproducibly, an increasing number of studies have employed lung slices to explore the interaction of hosts and pathogens (Chakrabarty et al., 2007; Londt et al., 2013; Punyadarsaniya et al., 2011; Seehase et al., 2012; Van Poucke et al., 2010; Wu et al., 2010). Recently, several studies have shown that pig lung slices can support influenza virus replication (Londt et al., 2013; Van Poucke et al., 2010). Another study demonstrated that influenza virus infection can induce robust cytokine and chemokine responses in human lung slices (Wu et al., 2010). Theoretically, the three-dimensional lung slice culture system can be used to evaluate the potency of both antiviral and anti-inflammatory agents against influenza virus infection.

In the current study, we showed that influenza viruses can efficiently replicate in mouse lung slices and induce significantly elevated levels of cytokines and chemokines. A panel of antiviral and anti-inflammatory agents were tested for their antiviral activities and/or anti-inflammatory effects in the mouse lung slices. The results from the lung slice model are consistent with those from mouse studies. Our results showed that the lung slice model provides a robust, convenient and cost-economical method for the screening and evaluation of both antiviral and anti-inflammatory agents against influenza virus infection in one assay.

2. Material and methods

2.1. Virus strains and animals

6–8-week old BALB/c mice were purchased from Changsha Laboratory Animal Center (Hunan province, China) and were housed under specific-pathogen-free condition. All experiments were conducted according to the protocol approved by the Animal Care and Use Committee of Wuhan Institute of Virology, Chinese Academy of Sciences (WIVA08201201).

Mouse adapted A/PuertoRico/8/34 (H1N1) and mouse adapted A/Human/Hubei/3/2005 (H3N2) were propagated in the allantoic cavity of 10-day-old specific-pathogen-free embryonated chicken eggs for 48 h. The allantoic fluids were collected and filtered with 0.22 μm filter and stored at −80 °C. The virus strains were provided by the virus collection at Wuhan Institute of Virology, Chinese Academy of Sciences, China.

2.2. Chemicals

15-deoxy-$\Delta^{12,14}$-prostaglandin J_2 (15d-PGJ_2), ribavirin and the neuraminidase substrate 2′-(4-methylumbelliferyl)-α-D-acetylneuraminic acid (MUNANA) were purchased from Sigma–Aldrich. EGCG was purchased from Sichuang Weikeqi Biological Technology Co. Ltd. (China). Glycyrrhizin was purchased from Shanghai Hanxiang Biological Technology Co. Ltd. (China). The P38 pathway inhibitor SB203580, the ERK pathway inhibitor U0126 and the SAPK/JNK pathway inhibitor SP600125 were purchased from Beyotime Institute of Biotechnology (China). Oseltamivir carboxylate (GS 4071) was obtained from Toronto Research Chemicals (Canada). All compounds were initially dissolved in dimethyl sulfoxide (DMSO, Sigma–Aldrich).

2.3. Preparation of the mouse lung slices

Mouse lung slices were prepared using a modification of a protocol that has been previously reported (Bauer et al., 2010). After anesthetisation by intraperitoneal injection of sodium pentobarbital (75 mg/kg), the mouse was bled through the abdominal aorta. Then, the trachea was exposed, dissected from surrounding tissues and was cannulated with an 18-gauge needle. Through the cannula, the lung was inflated with 1.3 ml of 2% low-melting agarose (BIO-RAD) dissolved in Hank's buffered saline solution (HBSS) solution. The whole animal was cooled with ice for 10 min to solidify the agarose and, thereby, the lung. Then, the lung was taken out *en bloc* from the thoracic cavity and placed in the slice culture medium (Dulbecco's Modified Eagle Medium: Nutrient Mixture F-12, DMEM/F-12, GIBCO) at 4 °C for an additional 15 min to completely solidify the agarose. The culture medium was supplemented with 100 units/ml of penicillin, 100 μg/ml streptomycin and 250 ng/ml of amphotericin to avoid contamination. The lung lobe was afterwards dissected and cut to create a flat surface at the end of the primary bronchus. Another flat surface was cut approximately 0.8 cm from the first surface. The cube was maintained in the pre-chilled slice culture medium prior to or during the slicing. The cube was cut into slices of desired thickness using a vibratome slicer (Leica, VT1200S). Each mouse lung cube generated at least 24 250-μm slices. The slices were then transferred into a 48-well cell culture plate and covered with 250 μl of slice culture medium in each well. The medium was changed every hour at least three times before virus infection to remove cell debris.

2.4. Slice viability

The lung slice viability was assessed by bronchoconstriction and live/dead staining. The bronchoconstriction was monitored under a microscope when adding or removing 10^{-4} M acetyl-ß-methylcholine chloride (Sigma–Aldrich). The photos were taken using a Nikon Inverted Research Microscope Ti ECLIPSE. For live/dead staining experiments, the slices were incubated with Calcein AM (1 μM) and Propidium Iodide (PI, 1 μg/ml) for 20 min at room temperature. A Nikon Multiphoton Confocal Microscope A1 MP^+ was used to record the images.

2.5. Infection of the lung slices with influenza viruses

The lung slices were infected with 200 μl of 10^5 PFU/ml influenza viruses for 2 h. Virus diluent was used as a negative control.

After the incubation, the viruses were discarded, and the slices were washed twice with phosphate buffered saline (PBS); then, fresh medium was added. At the indicated time points, the supernatants were harvested, and the virus titres and expression levels of cytokines and chemokines were detected. The slices were stored at −80 °C until RNA extraction was performed.

For the drug addition assay, 250-μm-thick lung slices were prepared as described in Section 2.3. After the last wash, the slices were infected with 200 μl of 10^5 PFU/ml PR8 virus. After incubation for 2 h, the virus was discarded, and the slice was washed with PBS. For the measurement of the Z′ factor, each 48-well plate (one lung slice per well) was processed as follows: one column was uninfected, one column was infected and mock treated, the rest of columns were infected and treated with 200 μl of six concentrations of 3-fold dilutions of ribavirin starting from 200 μM. In total, four plates were processed. For the lung slice model validation assay, each 48-well plate contained two agents, and each data point had three lung slices. NA activity and IP-10 level were determined 48 h post infection.

2.6. Measurement of virus titre

The virus titres were determined by a $TCID_{50}$ assay. Briefly, Madin-Darby Canine Kidney (MDCK) cells were maintained in DMEM supplemented with 10% foetal bovine serum and 100 units/ml of penicillin/streptomycin. MDCK cells were seeded into 96-well cell culture plates. Twenty-four hours later, 10-fold serial dilutions of the supernatant were inoculated on an MDCK monolayer at 37 °C for 72 h, and the cytopathic effects were examined. The virus titres were calculated by the Reed–Muench method (Reed and Muench, 1938).

2.7. Neuraminidase activity assay

2′-(4-Methylumbelliferyl)-α-D-acetylneuraminic acid (MUNANA) is a fluorometric substrate of the neuraminidase of the influenza virus. The virus containing sample was mixed with 20 μM MUNANA, which is dissolved in a MES solution (33 mM 2-[N-morpholino] ethanesulfonic acid and 4 mM $CaCl_2$, pH = 6.5), and incubated at 37 °C for 2 h in a 96-well black Optiplate (PerkinElmer). The reactions were stopped by adding 0.14 M NaOH in 83% ethanol, and the fluorescence signal was recorded at 355 nm (excitation) and 485 nm (emission) using the Wallac Envision Multilabel Reader (PerkinElmer).

2.8. Cytokine and chemokine analysis at protein level

The protein levels of TNF-α, IL-6, IL-10, IL-1β, IFN-γ, MIP-3α, IP-10, and RANTES were measured using commercial ELISA kits (BOSTER Biotechnology Company, Wuhan, China). For the anti-inflammatory assay using IP-10 as readout, the protein levels of IP-10 were measured using Duoset ELISA development kits (R&D).

2.9. MTT assay

Drug toxicity was assessed by MTT assay. The slices were incubated with 200 μl serially diluted concentrations of drugs for 48 h. Then the drugs were removed and the slices were washed once with PBS and incubated with MTT (0.5 mg/ml) for 40 min at 37 °C. After the formazan was completely dissolved in 200 μl of DMSO, 100 μl of DMSO solution was transferred to a 96-well plate. The optical density (OD) of the dissolved formazane was measured at 540 nm.

2.10. Immunofluorescence assay

The 150 μm thick lung slices were cut and exposed to 200 μl of 10^6 PFU/ml PR8 (H1N1) or HUBEI (H3N2) viruses. After incubation for 2 h, the viruses were removed and fresh medium were added. 24 h later, the slices were fixed with 4% paraformaldehyde for 2 h at room temperature. The slices were then incubated in blocking buffer (PBS containing 3% BSA, 1% Triton X-100 and 10% normal goat serum) for another 3 h. Afterwards, the slices were immunoprobed with antibody against nucleoprotein of influenza A virus (1:100, Santa Cruz sc-80481) and in binding buffer (PBS containing 3% BSA and 1% Triton X-100) overnight at 4 °C. After washing three times with PBS, the slices were incubated with DAPI (200 μg/ml, Sigma–Aldrich) and TRITC-conjugated goat anti-mouse IgG (1:100) for 1 h. Fluorescent images were obtained using a Nikon multiphoton Confocal Microscope A1 MP^+ (Nikon).

2.11. Total RNA extraction and real-time RT-PCR

Total RNA was extracted from lung slices with the E.Z.N.A™ MicroElute Total RNA kit according to the animal tissue protocol (Omega). Reverse transcription was conducted using a random hexamer primer. Real-time quantitative PCR was performed using the iTaq™ universal SYBR® Green supermix (BIO-RAD). The PCR conditions were 94 °C for 30 s and 40 cycles of 94 °C for 15 s and 60 °C 30 s. The primers for cytokines and chemokines were synthesised according to previously published data (Giulietti et al., 2001).

2.12. Animal experiment

Mice were anesthetized by intraperitoneal injection of sodium pentobarbital (75 mg/kg). Twenty microlitres of 10^5 PFU/ml PR8 virus was inoculated nasally. The mock group was inoculated with virus diluent. On day 3 post infection, the mock mice and infected mice were sacrificed The tracheas and lungs were removed and washed three times with an injection of 2 ml of PBS containing 0.1% BSA. After centrifugation at 3000 rpm, the bronchoalveolar lavage fluids (BALF) were stored at −80 °C.

2.13. Statistical analysis

Statistical analysis was performed by the unpaired *t*-test. Correlation of cytokines/chemokines between *ex vivo* and *in vivo* was evaluated using a linear regression analysis using GraphPad Prism 5.0 software. CC_{50} and EC_{50} values were determined using non-linear regression using GraphPad Prism 5.0. Statistical significance was determined as follows: *, $0.01 < p < 0.05$; **, $0.001 < p < 0.01$. The data in the figures are represented as the means ± SEM. The Z′ factor was calculated according to the method described previously (Zhang et al., 1999).

3. Results

3.1. Mouse lung slices remain viable for at least 5 days ex vivo

To establish the *ex vivo* lung slice model for influenza virus infection, the viability of lung slices must be maintained. We first tested how long the mouse lung slices can remain viable under the *ex vivo* culture condition. Mouse lung slice viability was assessed based on the bronchoconstriction assay and live/dead viability assay. As shown in Fig. 1, a strong bronchoconstriction (compare A with B) could be induced on days 1, 3 (data not shown) and 5 after treatment with 0.1 μM acetyl-ß-methylcholine chloride. The removal of the drug resulted in relaxation of the airway (Fig. 1C). To further assess the viability of lung slices, the live/dead

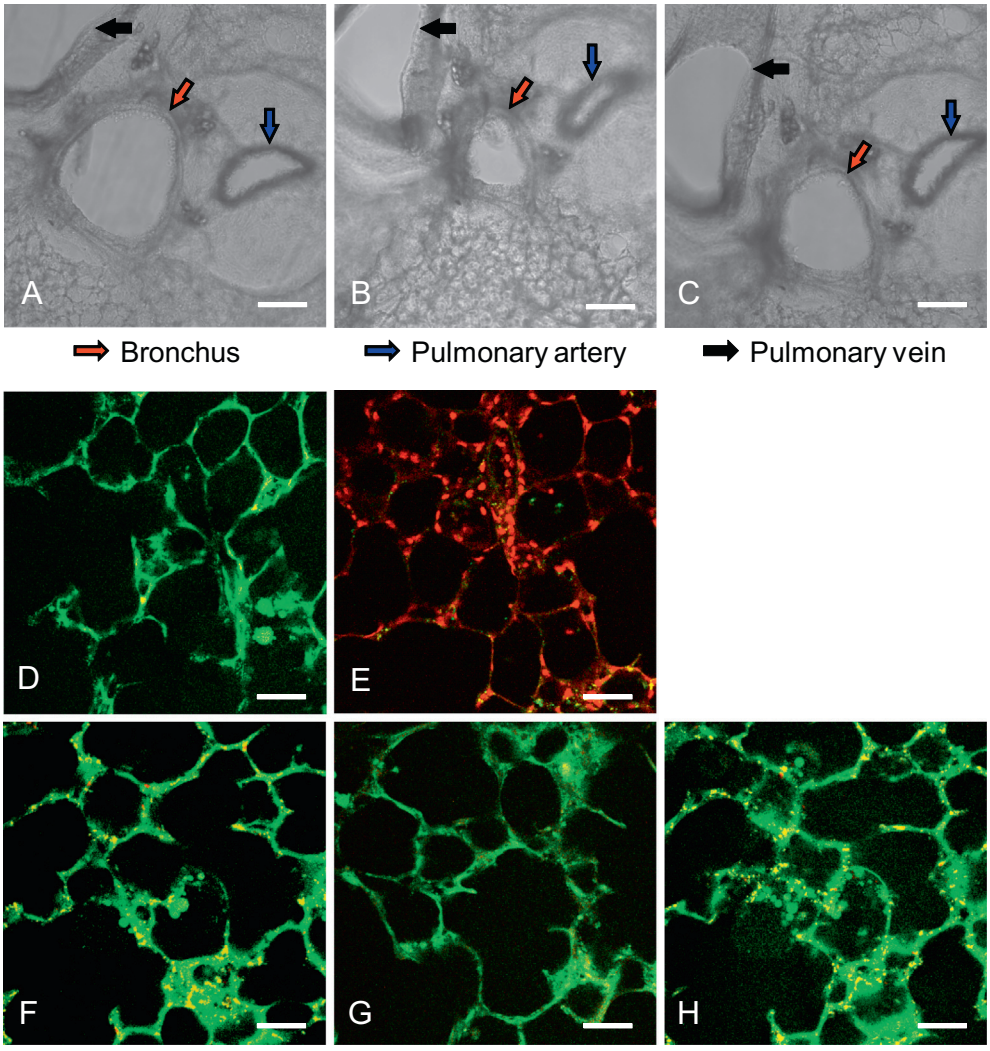

Fig. 1. Mouse lung slices remain viable for at least 5 days *ex vivo*. (A–C) The 250-μm thick lung slices were prepared, and the bronchoconstriction was observed 5 days after preparation. The untreated slices (A) were incubated with 0.1 μM acetyl-ß-methylcholine chloride at 37 °C for 5 min (B) in a 24-well cell culture plate. Then, the drug was removed, lung slices were washed twice with PBS and incubated with fresh culture medium at 37 °C for 10 min (C). The images were captured using a Nikon's Eclipse Ti inverted microscope. Red, blue and black arrows show the lung bronchus, pulmonary artery and pulmonary vein, respectively. Scale bar = 200 μm. (D–H) Live/dead staining assay. Lung slices were stained with Calcein-AM (1 μM) and Propidium Iodide (PI, 1 μg/ml) for 20 min at room temperature on days 1, 3 and 5 after preparation (lower panels, F–H). The middle panel shows a viable slice directly after preparation (D), and a slice with complete loss of activity (treated by 1% Triton-100) (E) for comparison. Calcein-AM and PI were used to simultaneously determine the live and dead cells. After being washed twice with PBS, images were taken using a Nikon multiphoton Confocal Microscope A1 MP$^+$ with excitation at 800 nm, and an emission filter of 500/50 nm for Calcein-AM and 625/50 nm for PI. Scale bar = 50 μm. (For interpretation of the references to colour in this figure legend, the reader is referred to the web version of this article.)

staining method was used to evaluate whether the alveolar architecture remained intact and alive after preparation and *ex vivo* culture. As shown in Fig. 1, the slices were almost 100% green (viable cells) directly after preparation (Fig. 1D), whereas treatment of the slices with 1% Triton-100 resulted in only red nuclei staining (dead cells, Fig. 1E). In addition, the mouse lung slices stayed alive and the alveolar architecture in lung slices remained intact up to 5 days after preparation (Fig. 1F–H). Collectively, these results suggest that the mouse lung slices can be kept alive for at least 5 days after preparation.

3.2. Mouse lung slices support influenza virus replication

Because the lung slices can survive under *ex vivo* conditions, we assessed whether influenza viruses can infect and replicate in the mouse lung slices. First, lung slices with different thicknesses were generated to determine the optimal thickness of lung slice suitable for the infection of influenza viruses. As expected, 250-μm thick slices produced more infectious virions 48 h post-infection than 125-μm thick slices. However, the virus yields of 500 and 1000-μm thick slices were similar to those of 250-μm thick slices (Fig. 2A). These results suggest that 250-μm thick lung slices are the best for infection with influenza virus, balancing cost and efficiency. Next, the growth curves of influenza viruses in mouse lung slices were obtained. As shown in Fig. 2D and E, both PR8 (H1N1) and HUBEI (H3N2) viruses demonstrated time-dependent replication and reached their maximum titre 48 h post infection, though the virus titres *ex vivo* are much lower than those in cell culture. Neuraminidase (NA) activity results (Fig. 2B and C) showed that both virus strains have similar kinetics in virus replication and infectivity (Fig. 2D and E), suggesting that NA activity can precisely represent the virus replication and infectivity in lung slices. To further correlate NA activity and virus titre, ribavirin and U0126 were tested for dose dependent inhibition. As shown in Fig. S1, both compounds exhibit dose dependent inhibition of NA activity or virus infectivity, indicating that NA activity can be used to

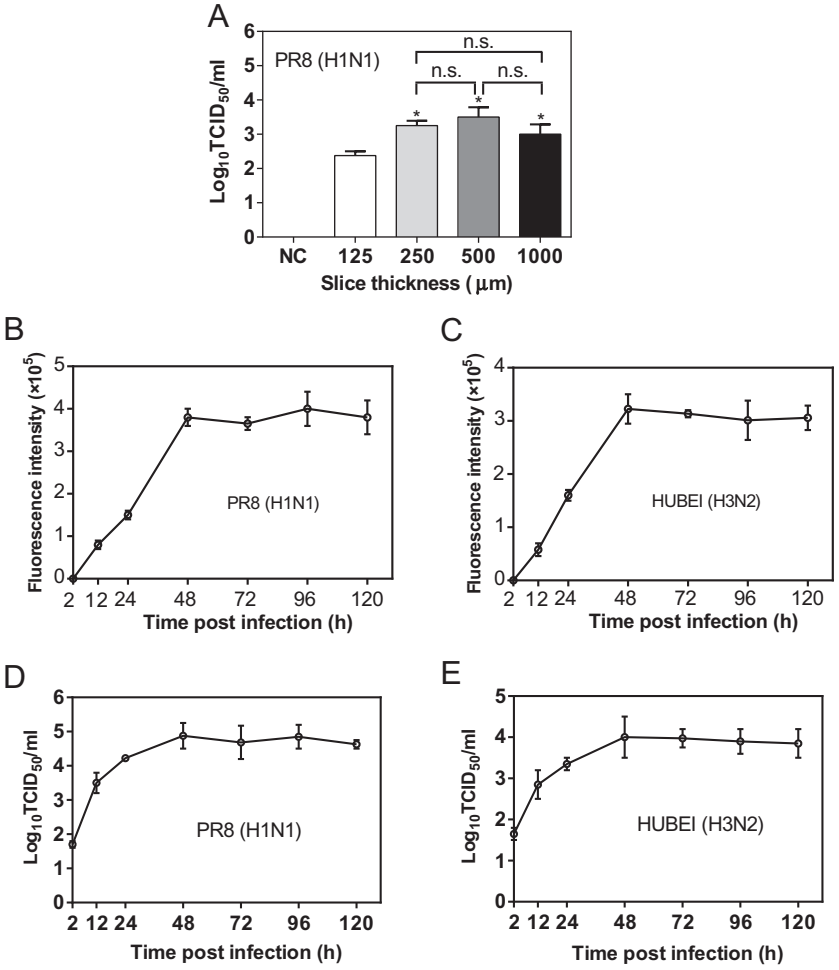

Fig. 2. Mouse lung slices support influenza virus replication. (A) To determine the virus production of lung slices of different thickness, 125-, 250-, 500- and 1000-μm thick lung slices were exposed to 200 μl of 10^5 PFU/ml of PR8 (H1N1) for 48 h, and the supernatants were used to determine the virus titre by a $TCID_{50}$ assay. Comparisons between groups were performed by an unpaired *t*-test. Data are expressed as the means ± SEM. n.s., non-significant. *, $0.01 < p < 0.05$ in comparison to 125-μm thick slices. (B–E) To determine the virus yields at different time points post infection, 250-μm thick slices were infected with 200 μl of 10^5 PFU/ml PR8 (H1N1) (B, D) or HUBEI (H3N2) (C, E) virus. The supernatants were collected at indicated time points to perform the NA activity assay (B and C) and $TCID_{50}$ assay (D and E). (F) Infection of lung slices was assessed by the IFA assay. Slices with a thickness of 150 μm were exposed to 200 μl of 10^6 PFU/ml PR8 (H1N1) or HUBEI (H3N2) viruses for 24 h. The slices were fixed with 4% paraformaldehyde and analysed by IFA. The images were captured using a Nikon multiphoton Confocal Microscope A1 MP^+. The virus diluent was used as a negative control (NC) in the infection. Scale bar = 1000 μm. The right panels show enlarged regions of interest from the left panels.

represent virus replication in the primary screening. To further confirm the infection of the lung slices by influenza virus, an immunofluorescence assay (IFA) was used to stain the nucleoprotein (NP) of influenza virus on the lung slices. As shown in Fig. 2F, the lung slice was strongly infected by influenza virus. Overall, these results demonstrated that lung slices support influenza virus replication.

3.3. Cytokine and chemokine responses following influenza virus infection in mouse lung slices

One aim of our study was to evaluate the anti-inflammatory effects of potential agents in lung slices. Many cytokines and chemokines are elevated in influenza-infected mice and seem important in influenza-induced inflammation. Despite complications in the cytokine storm induced by influenza virus infection, we chose eight important cytokines and chemokines (Belisle et al., 2010; Brandes et al., 2013; Lauder et al., 2013; Szretter et al., 2007; Wang et al., 2013; Weiss et al., 2010) to study the inflammatory response following influenza virus infection. First, we examined the mRNA levels of cytokines and chemokines in influenza virus-infected lung slices by real time RT-PCR. As shown in Fig. 3A and B, exposure to 10^5 PFU/ml doses of PR8 and HUBEI viruses resulted in elevated mRNA levels of most cytokine and chemokine genes tested. At 12 h post infection, the gene transcriptions were elevated and were highly activated at 48 h post infection. The cytokines and chemokines with the highest levels of induction in transcription by both viruses were RANTES and IP-10. Because the cytokine and chemokine responses mediated by the two viruses at transcription level are similar, the PR8 influenza virus was used for the steady protein level analysis. We then further determined the protein levels of selected cytokines and chemokines in response to influenza virus infection at 24 h and 48 h post infection. As shown in Fig. 3C, after exposure to PR8 virus for 24 h, the protein levels of all tested cytokines and chemokines were significantly elevated except for IL-1β and IL-10. IFN-γ was undetectable in the supernatant of the lung slices. The fold increase over mock for TNF-α, MIP-3α, IL-6, RANTES and IP-10 were 2.1, 3.3, 2.4, 1.7 and 8.9, respectively. At 48 h post infection, higher levels of cytokines and chemokines were induced (Fig. 3D), and the fold increases were 4, 4.4, 3, 4 and 19, respectively. IP-10 was the most highly stimulated chemokine at both 24 h and 48 h post infection, which is consistent with the results of its mRNA response to virus infection. Taken together, our results suggest that a strong

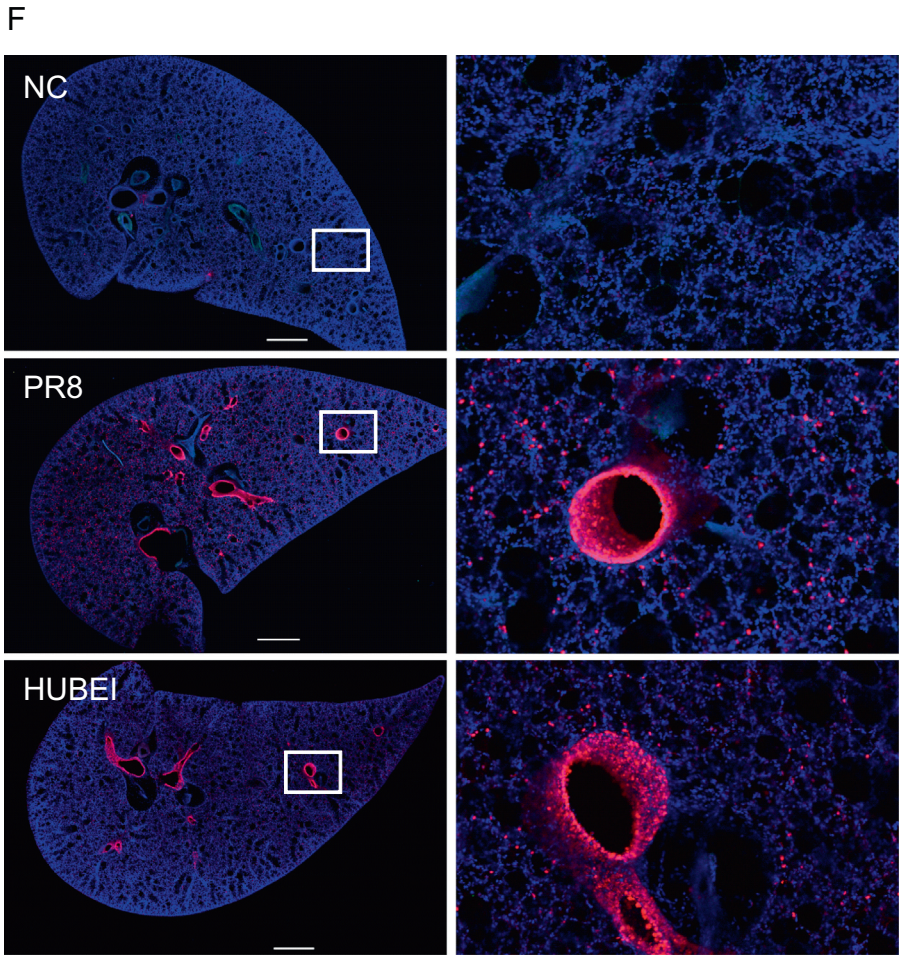

Fig. 2 (*continued*)

inflammatory response represented by the highly elevated mRNA and protein levels of cytokines and chemokines are triggered by the infection of influenza viruses in the *ex vivo* mouse lung slice.

3.4. Comparison of the cytokine and chemokine levels in response to influenza virus infection between ex vivo and in vivo models

Our results demonstrated that the *ex vivo* model supports influenza virus infection (Section 3.2) and exhibits an inflammatory response following influenza virus infection (Section 3.3). To meet the goal of this study in the establishment of an *ex vivo* mouse slice model for the screening and evaluation of both antiviral and anti-inflammatory drugs against influenza infection in one assay, ensuring that the *ex vivo* model has similar patterns in influenza-induced cytokine and chemokine responses is critical. As shown in Fig. S2, the inflammatory responses *in vivo* on day 3 post-infection appeared to be most robust. The cytokine/chemokines levels *in vivo* on day 3 were chosen to compare with that *ex vivo*. The results from mouse studies showed that IFN-γ, IL-1β, TNF-α, and IL-10 exhibited lower levels of activation (181 pg/ml, 115 pg/ml, 198 pg/ml and 278 pg/ml, respectively), whereas MIP-3α, IL-6, RANTES and IP-10 exhibited higher levels of activation in bronchoalveolar lavage fluid (BALF, 625 pg/ml, 982 pg/ml, 1216 pg/ml and 5000 pg/ml, respectively). The elevated expression of most of the tested cytokines and chemokines in the supernatant of lung slices demonstrated the same expression pattern compared with that in the mouse model (Figs. 3C, D and 4A). To evaluate the correlation between *ex vivo* and *in vivo* levels of cytokines and chemokines, a linear regression analysis model was employed. The levels of cytokines and chemokines in the supernatants of the lung slices 24 h post infection (Fig. 3C) were compared to that in the BALF of mice 3 day post infection. The results show that there is a positive correlation between *ex vivo* and *in vivo* expression of selected cytokines and chemokines with a coefficient of correlation of 0.75 (Fig. 4B). More specifically, IP-10, RANTES and MIP-3α are perfectly correlated. The coefficient of correlation between cytokines and chemokines in the supernatant of lung slices 48 h post infection (Fig. 3D) and that in the BALF of mice 3 day post infection was 0.61 (Fig. S3). Our results here demonstrated that the *ex vivo* mouse lung slice model resembles the *in vivo* mouse model in response to influenza virus infection. In addition, IP-10, RANTES and MIP-3α may serve as readouts in the screening and evaluation of anti-inflammatory agents against influenza infection.

3.5. Assay performance for antiviral and anti-inflammatory activities in the mouse lung slice model

To assess the quality of the mouse lung slice model, we used ribavirin, an antiviral drug, as a reference in a pilot experiment to test the Z′ factors for the measurements of antiviral and anti-inflammatory activities. The Z′ factor, a screening window coefficient, can be used to evaluate the quality of assays (Zhang et al., 1999). Neuraminidase was chosen as a readout for antiviral activity, which was confirmed to correlate well with the production of infectious virions (Fig. 2B–E). IP-10 was chosen as a readout

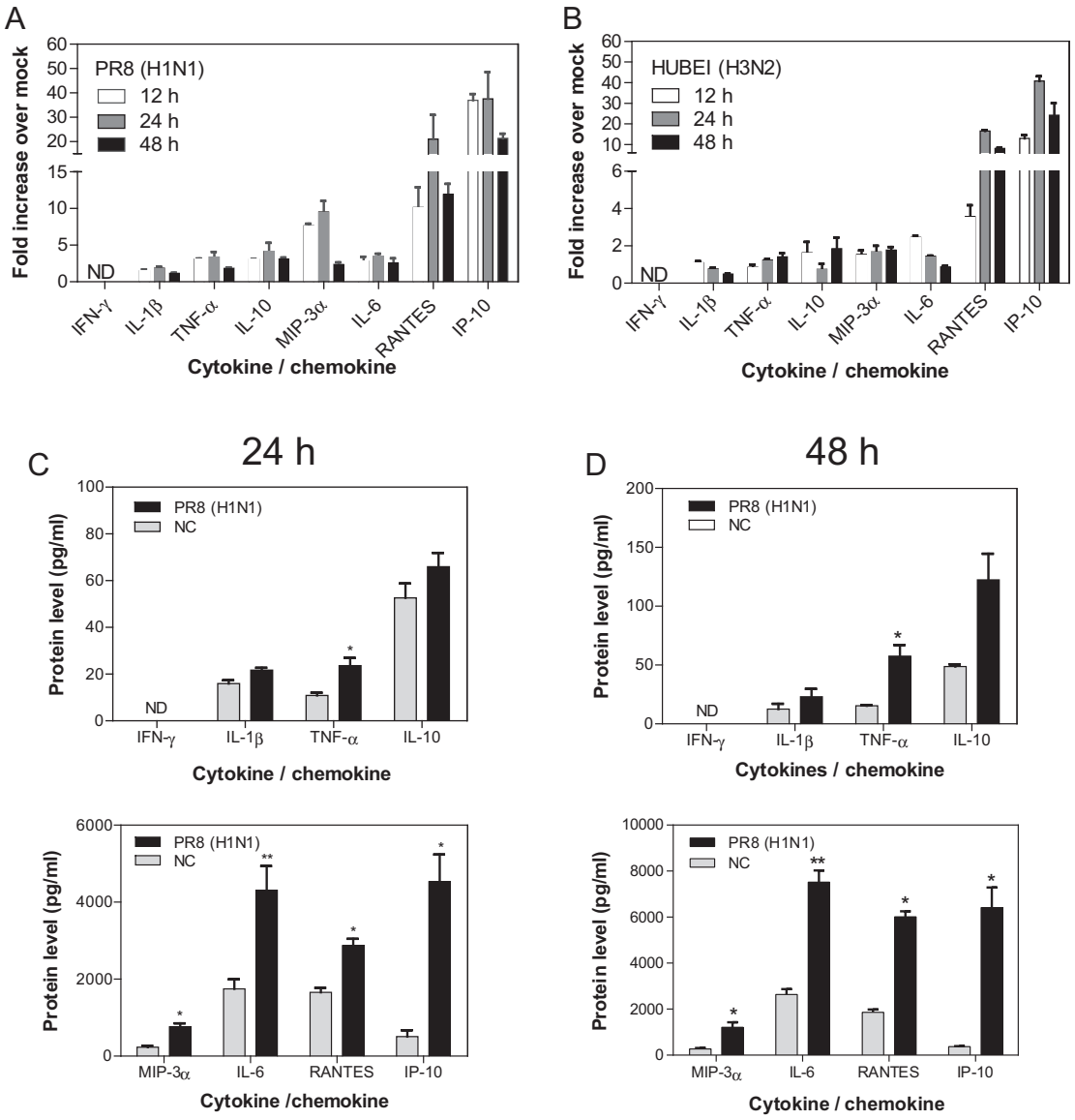

Fig. 3. The cytokine and chemokine responses induced by influenza virus infection of mouse lung slices. (A, B) The analysis of the mRNA levels of selected cytokines and chemokines. Following infection by 200 μl of 10^5 PFU/ml of PR8 (H1N1) (A) and HUBEI (H3N2) (B), lung slices were collected at indicated times post infection and were lysed to quantify the mRNA levels of cytokines and chemokines by real time RT-PCR. Each data point was from three lung slices and virus diluent was used as a negative control. The gene expression normalised to β-actin mRNA was shown as fold expression values over negative control. The data were analysed using the $2^{-\Delta\Delta Ct}$ method. The data are expressed as the means ± standard error of the means (SEMs). (C, D) The analysis of the protein levels of selected cytokines and chemokines. Following exposure to 200 μl of 10^5 PFU/ml of PR8 (H1N1) virus, the supernatants were sampled at 24 h (C) and 48 h (D) post infection and were used to determine the protein levels of cytokines and chemokines by ELISA. To show the induced changes, cytokines and chemokines were placed in separate panels according to scales of the protein levels. Each data point was from three lung slices, and virus diluent was used as a negative control. Comparisons between the infected group and the negative control were performed by the unpaired *t*-test (*, $0.01 < p < 0.05$; **, $0.001 < p < 0.01$). The data are expressed as the means ± SEM. ND, not detected (for real-time PCR, no amplification was detected during the 40 cycles. For ELISA, the signal was below the detection limit of the commercial kit).

to represent the influenza virus-induced inflammation for three reasons: (a) it exhibits good correlation between *in vivo* and *ex vivo* models at the protein level, (b) it is the most highly induced chemokine in the mouse model and in the lung slice model, and (c) IP-$10^{-/-}$ mice or mice treated with anti-IP-10 antibody demonstrate global down-regulated cytokines and chemokines and can survive after challenged by a lethal dose of influenza virus (Wang et al., 2013). Therefore, ribavirin was used to determine its NA and IP-10 inhibition effects to test the performance of the lung slice model. Four replicate plates were processed to determine the Z′ factor. As shown in Table 1, a Z′ factor ranging from 0.53 to 0.71 for NA inhibition and 0.58 to 0.73 for IP-10 inhibition demonstrated that the quality of the lung slice model for the evaluation of both antiviral and anti-inflammatory effects is satisfactory.

3.6. The validation of the mouse lung slice model using a panel of antiviral and anti-inflammatory agents with known activities in vivo

To further validate our mouse lung slice model, a panel of agents with known antiviral or anti-inflammatory activities *in vivo* was tested for antiviral and anti-inflammatory effects in the lung slice model. Among these agents, ribavirin, oseltamivir and gemacrone are anti-influenza drugs. EGCG and U0126 have both antiviral and anti-inflammatory effects *in vivo*. 15d-PGJ_2 and SB203580 have anti-inflammatory activities *in vivo*. All of these

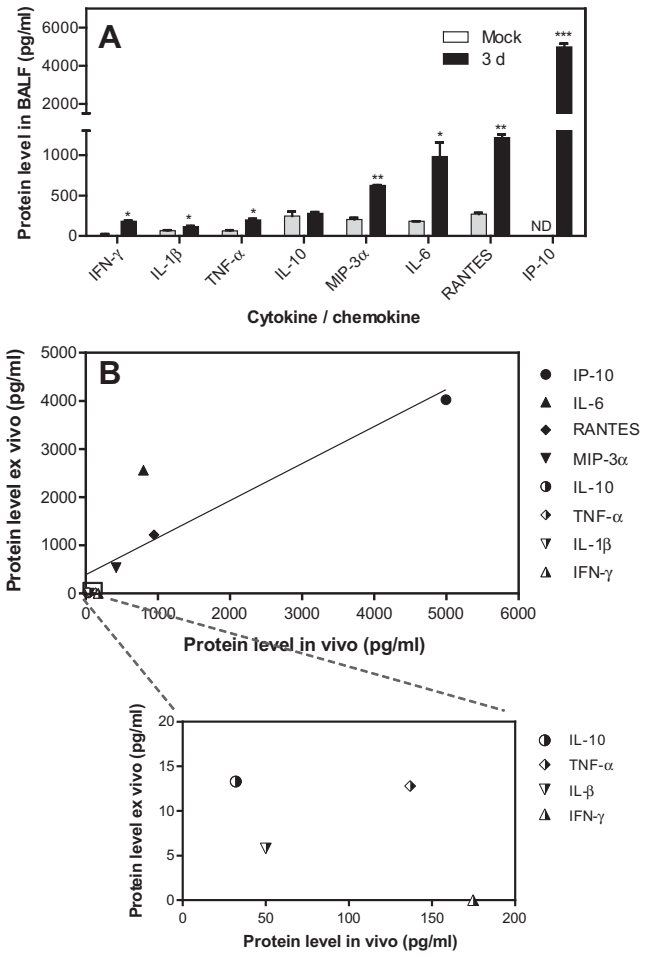

Fig. 4. Correlation analysis of the cytokine and chemokine levels in response to influenza infection between the *ex vivo* and *in vivo* models. (A) The cytokine and chemokine levels in response to influenza infection *in vivo*. The bronchoalveolar lavage fluids (BALF) were subjected to cytokine and chemokine measurement by ELISA. Comparisons between infected mice and mock mice were performed by the unpaired *t*-test (*, $0.01 < p < 0.05$; **, $0.001 < p < 0.01$). The data are expressed as the means ± SEM. ND, not detected (the signal was below the detection limit of the commercial kit). (B) Comparison of the cytokine and chemokine levels in response to influenza infection between the *ex vivo* and *in vivo* models. After subtraction of the corresponding levels of the mock group, the correlation of the virus-induced IL-1β, IFN-γ, TNF-α, IL-10, MIP-3α, IL-6, RANTES and IP-10 in BALF of day 3 post infection (Fig. 4A) and lung slice supernatants (Fig. 3C) were analysed by a linear regression analysis model.

agents have been reported to protect mice from death against lethal influenza infection. As shown in Table 2, all of the antiviral agents (ribavirin, oseltamivir, and gemacrone) efficiently inhibited virus replication in the lung slices, and the IP-10 levels were decreased as a result of the inhibition of viral replication (Fig. S4). Unexpectedly, oseltamivir inhibited only virus replication in the lung slices without interfering with IP-10 expression (Fig. S4).

In addition to their antiviral effects, U0126 and EGCG possess anti-inflammatory effects (Droebner et al., 2011; Ling et al., 2012; Pinto et al., 2011; Ranjith-Kumar et al., 2010). We found that both U0126 and EGCG can dose dependently decrease NA levels and IP-10 levels in the lung slice model. 15d-PGJ_2 and SB203580 were chosen because they protect mice from influenza infection by anti-inflammatory effects only (Borgeling et al., 2014; Cloutier et al., 2012). As expected, both 15d-PGJ_2 and SB203580 dose dependently decreased IP-10 levels, whereas neither inhibited virus replication in lung slices, suggesting they improved mouse survival through their anti-inflammatory mechanisms (Fig. S4).

To further validate the model, we also tested six agents (dicyclomine, clotrimazole, fenofibrate, proadifen, benzydamine and nafronyl oxalate) with known antiviral activity in MDCK cells (An et al., 2014) that failed to protect mice from lethal doses of influenza virus infection (Fig. S5). Results showed that dicyclomine, clotrimazole, fenofibrate, proadifen and benzydamine inhibited neither viral replication represented by NA activity nor inflammatory response represented by IP-10 levels in mouse lung slices (Fig. S4). However, nafronyl oxalate, although not showing any antiviral activity, inhibited the inflammatory response (with IP-10-EC_{50} of 22.1 μM, Fig. S4), although it did not improve mouse survival rate (Fig. S5).

Taken together, our results suggest that with the benefits of avoiding the overuse of animals and expensive compounds, the mouse lung slice model is robust and cost-efficient for screening and evaluating both antiviral and anti-inflammatory drugs against the influenza infection in one assay. Overall, the mouse lung slice can serve as a predictive model of the efficacy of drug candidates on the mouse model.

4. Discussion

Current anti-influenza drug screening is based primarily on transformed cells in the form of cell-based assays. Though the transformed cells are convenient for high throughput screening and the *in vitro* study of potency and mechanisms, they are distantly related to physiological and pathological conditions. As a consequence, results based on transformed cells may suffer from simplification. Current treatments for influenza rely on the use of antiviral drugs; however, the window for antiviral therapy is narrow. Several reports have shown that anti-inflammatory agents can be effective in reducing the death rate against the infection of lethal influenza (Borgeling et al., 2014; Cloutier et al., 2012).

Table 1
The pilot experiment of lung slices model using ribavirin. 250 μm thick lung slices were prepared as described in Section 2.3. The lung slices were infected with 200 μl of 10^5 PFU/ml PR8 virus. After 2 h incubation on 37 °C, the viruses were discarded and the lung slices were washed twice with PBS. Then six concentrations of ribavirin starting from 200 μM and with 3-fold serial dilution were added. NA activities and IP-10 levels in culture supernatants were determined 48 h post infection as described in Sections 2.7 and 2.8.

Plates	S/B-NA[a]	S/B-IP-10[b]	Z′-NA[c]	Z′-IP-10[d]	NA-EC_{50} (μM)[e]	IP-10-EC_{50} (μM)[f]
1	8.3	10.2	0.67	0.73	32.5	21.8
2	6.2	6.7	0.53	0.68	25.4	17.8
3	9.3	8.6	0.63	0.58	28.3	20.6
4	7.8	7.3	0.71	0.64	17.7	14.2

[a] S/B-NA: Signal to background for NA activity. Refer to ratio of NA signal in infected control wells to negative control wells.
[b] S/B-IP-10: Signal to background for IP-10 release. Refer to ratio of IP-10 in infected control wells to negative control wells.
[c] Z′-NA: Z′ factor for NA inhibition.
[d] Z′-IP-10: Z′ factor for IP-10 inhibition.
[e] NA-EC_{50}: 50% effective concentration determined by NA inhibition.
[f] IP-10-EC_{50}: 50% effective concentration determined by IP-10 inhibition.

Table 2
The evaluation of a panel of antiviral and anti-inflammatory agents in mouse lung slice model. The 250 μm thick lung slices were prepared as described in Section 2.3. The slices were infected with 200 μl of 10^5 PFU/ml PR8 virus. After 2 h incubation on 37 °C, the viruses were removed and the lung slices were washed twice with PBS. Then drugs with serially diluted concentrations were added and maintained for 48 h, and the NA activities and IP-10 levels were determined as described in Sections 2.7 and 2.8.

Chemical name	CC_{50}[a]	NA-EC_{50}[b]	IP-10-EC_{50}[c]	*In vivo*[d]	Possible mechanism[e] and Ref.[h]
Ribavirin	>200	32.5	21.8	+[g]	Antiviral (Zarogiannis et al., 2012)
Oseltamivir	>200	0.21	–[f]	+	Anti-influenza (Ilyushina et al., 2008)
Gemacrone	135.3	23.1	17.6	+	Anti-influenza (Liao et al., 2013)
U0126	72.3	12.03	1.3	+	ERK inhibitor (Pinto et al., 2011)
EGCG	>500	50.1	3.3	+	Antioxidant (Ling et al., 2012)
15d-PGJ_2	21.7	–	0.2	+	PPAR-γ agonist (Cloutier et al., 2012)
SB203580	>100	–	15.1	+	P38 inhibitor (Borgeling et al., 2014)
Dicyclomine	65.2	–	–	–	Antispasmodic
Clotrimazole	16.3	–	–	–	Antifungal
Fenofibrate	>200	–	–	–	PPAR-α agonist
Benzydamine	112.6	–	–	–	Anti-inflammatory
Proadifen	32.2	–	–	–	Cytochrome P450 inhibitor
Nafronyl oxalate	121.7	–	22.1	–	5-HT2 receptor antagonist

[a] CC_{50}: 50% cytotoxic concentration (μM) determined by the MTT assay.
[b] NA-EC_{50}: 50% effective concentration (μM) determined by NA activity assay.
[c] IP-10-EC_{50}: 50% effective concentration (μM) determined by ELISA of IP-10.
[d] *In vivo*: the protection effect of mice from lethal influenza infection.
[e] Possible mechanism: possible mechanism of the compound as stated on either its "label" or literature.
[f] –: no effect for virus inhibition, IP-10 inhibition or mice protection.
[g] +: agents can protect mice against lethal influenza virus infection according to the literature.
[h] Ref.: the reference of the reported protection effect of antivirals or anti-inflammatory agents *in vivo*.

Moreover, current antiviral drug screening is performed primarily using cell-based assays. The cell-based assays available for the development of anti-inflammatory agents against influenza virus infection are largely targeting single host factors or pathways that play a role in the influenza-induced inflammatory response. Such strategies could be very risky for the development of anti-inflammatory drugs and lead to failure in animal tests or in clinical trials. Whereas animal models, e.g., mice and ferrets, are good for efficacy studies in of both antiviral and anti-inflammatory drugs, they are not time- or cost-efficient. To overcome this problem, at least in part, we have established the mouse lung slice model to test drugs for antiviral and anti-inflammatory activities in one *ex vivo* assay with the convenience of the *in vitro* cell-based assay. The goals for this model are as follows: (i) the mouse slices can remain alive long enough for efficient influenza virus infection and inflammatory response; (ii) the inflammatory response is similar to that in the lung of mouse; (iii) to choose the best readouts for the antiviral and anti-inflammatory activities in the model; and (iv) to validate the model using antiviral and anti-inflammatory agents with confirmed efficacy *in vitro* and *in vivo*.

The tissue viability of the lung slices was the first concern in establishing the lung slice model. Mouse lung slices can survive and maintain their native structure for at least three days after preparation (Sanderson, 2011; Siminski et al., 1992). The methods to monitor the viability of lung slices include the measuring of the LDH release, ciliary activity, bronchoconstriction induced by stimuli, and live/dead staining (Sanderson, 2011). In our research, results from bronchoconstriction experiments and live/dead staining experiments demonstrated that lung slices remained alive for at least 5 days. Moreover, the infection of lung slices by influenza viruses and the kinetics of virus growth are better indications that the mouse lung slices stay viable for at least the first 2 days after preparation.

Our second goal was to establish an *ex vivo* model for the infection of mouse lung slices by influenza viruses and the induction of inflammatory responses similar to that in the mouse model. Our results demonstrated that influenza viruses replicate efficiently in the mouse lung slices. These results are consistent with previous reports showing that the influenza virus can replicate in pig lung slices (Van Poucke et al., 2010). By IFA, mouse lung slices were clearly shown to be infected by influenza virus. To analyse the inflammatory response of lung slices following the infection of the influenza virus, we measured the levels of cytokine and chemokine and compared them with those in the BALF of mice. Our results showed that a positive correlation exists between the *ex vivo* and *in vivo* models in the expression of selected cytokines and chemokines with a coefficient of correlation of 0.75. IFN-γ and IL-1β were significantly induced *in vivo* but not *ex vivo*. This may be due to an influx of multiple types of immune cells in the lung *in vivo* but not in the lung slice. The lower levels of IL-1β in lung slices may be due to the observation that the epithelial cells and macrophages secreted less IL-1β than neutrophils in responds to influenza infection (Brandes et al., 2013). The observation that IFN-γ secretion was not detected in lung slices can be explained by the fact that the primary source of IFN-γ are NK cells, $CD4^+$ Th1 cells and $CD8^+$ T cells (Schroder et al., 2004), which are absent in the lung slice. Despite the discrepancy in some of the cytokine and chemokine responses, IP-10, RANTES and MIP-3α are perfectly correlated between the *ex vivo* and *in vivo* models. Therefore, IP-10, RANTES and MIP-3α may represent the inflammatory response following influenza virus infection in the *ex vivo* model.

The choice of readout for antiviral effects is straight forward and was determined previously in our lab. The fluorometric substrate of the neuraminidase of the influenza virus, MUNANA, is used for detection of virus neuraminidase activity, which represents the levels of virus replication (An et al., 2014). The virus replication level determined by NA activity is proportional to that of the $TCID_{50}$ as shown in Fig. 2 (compare 2B and 2D, 2C and 2E). However, the choice of readout for anti-inflammatory activity is much more complicated because no known cytokine or chemokine is widely accepted to represent the inflammatory response to influenza infection. Based on the comparison between *ex vivo* and *in vivo* responses of the selected cytokines and chemokines following influenza virus infection, IP-10, RANTES and MIP-3α may serve as readouts for influenza-induced inflammation. In the recent literature, to elucidate which cytokine and chemokine is more important in the influenza-induced innate immune response, cytokines or their receptor gene were knocked out in mice. $TNFR1^{-/-}$, $IL\text{-}6^{-/-}$, $MCP\text{-}1^{-/-}$, $IL\text{-}1R^{-/-}$, $MIP\text{-}1^{-/-}$, $CCR2^{-/-}$, and $GM\text{-}CSF^{-/-}$ mice did not survive influenza infection; however, $IP\text{-}10^{-/-}$ mice did survive influenza infection, suggesting that IP-10 may play an

important role in the aberrant cytokine responses during influenza infection (Darwish et al., 2011; Wang et al., 2013). IP-10 has also been proposed to be a poor prognostic indicator for patients with severe acute respiratory syndrome (SARS), which is clinically similar to severe influenza infection (Nelli et al., 2012). Although we did not compare the proteome changes induced by influenza, the rationale to choose a single factor to prove the concept has been previously reported (Cameron et al., 2008). Taking these results into consideration, we chose IP-10 as a readout for the evaluation of anti-inflammatory drugs, and IP-10 appeared to be valid for representing the inflammatory response in the validation test of a panel of antiviral and anti-inflammatory agents. Of course, if a critical study of the efficacy of a candidate compound is required, multiple readouts determined by the levels of multiple cytokines and chemokines can be used to assess the inhibitory effects against the inflammatory response following influenza virus infection.

Very often, compounds showing antiviral or anti-inflammatory activity in the single cell system fail in the animal assay. To validate this precision cut mouse lung slice model in screening and evaluation of both antiviral and anti-inflammatory drugs against influenza virus infection in one assay using NA and IP-10 as readouts, four categories of known antiviral and anti-inflammatory drugs were tested for their antiviral and anti-inflammatory activities. The results were compared with that from mouse studies conducted by others and us. The four categories of agents are: (i) agents with only antiviral effects *in vitro* and *in vivo*; (ii) agents with both antiviral and anti-inflammatory effects *in vitro* and *in vivo*; (iii) agents with only anti-inflammatory effects *in vitro* and *in vivo*; (iv) agents with antiviral effects *in vitro* which failed in the mouse model. The agents of the first three categories showed antiviral or anti-inflammatory effects in the lung slice model. Among the agents from the category IV, all failed to show any antiviral or anti-inflammatory activity on the mouse lung slice model, except that nafronyl oxalate was shown to inhibit IP-10 release. Overall, this validation testing of a group of agents with known antiviral or anti-inflammatory activities demonstrated that the mouse lung slice model is valid, convenient and cost-efficient for screening and evaluation of both antiviral and anti-inflammatory drugs in one *ex vivo* assay. It appears that only drugs showing either antiviral or anti-inflammatory activity in the mouse lung slice model may protect mice from infection of lethal influenza, though exceptions may occur.

In summary, we established and validated a mouse lung slice model to evaluate compounds for antiviral and anti-inflammatory effects in one assay. Importantly, employing the lung slice model is economical in term of experiment costs, in compound synthesis and animal use. For the development of antiviral drugs, the mouse lung slice model is more similar to the mouse model. For the development of anti-inflammatory drugs, the mouse lung slice model is suitable for drugs targeting multiple targets and pathways involved in the inflammatory response following influenza infection and more similar to the mouse model. This model can be useful in the secondary screening for selection of drug candidates with potent antiviral or (and) anti-inflammatory activities before testing in an animal model.

Notably, the mouse lung slice model should be used with caution in testing anti-inflammatory drugs against influenza viruses other than H1N1 in two aspects. Firstly, to make sure that the virus being tested can replicate efficiently on mouse lung slices and induce cytokine/chemokine responses similar to that *in vivo*. Secondly, the readout(s) for the inflammatory response can be different and should be determined experimentally *ex vivo* and *in vivo*. Considering that the infection of many respiratory viruses causes acute inflammation in the human lungs and induce similar inflammatory responses, it is likely that the anti-inflammatory drugs developed using the influenza virus infected mouse lung slice model may also be effective in the treatment of infection of other respiratory viruses.

Taken together, our research demonstrates that it is beneficial to use the mouse lung slice model to develop new drugs with either antiviral or anti-inflammatory activities in the treatment of influenza virus infection.

Acknowledgments

This work was jointly funded by the National Basic Research Program of China (2009CB522504), the Important National Science & Technology Specific Projects (2009ZX09301-014).

Appendix A. Supplementary data

Supplementary data associated with this article can be found, in the online version, at http://dx.doi.org/10.1016/j.antiviral.2015.05.008.

References

An, L., Liu, R., Tang, W., Wu, J.G., Chen, X., 2014. Screening and identification of inhibitors against influenza A virus from a US drug collection of 1280 drugs. Antiviral Res. 109, 54–63.

Bauer, C.M., Zavitz, C.C., Botelho, F.M., Lambert, K.N., Brown, E.G., Mossman, K.L., Taylor, J.D., Stampfli, M.R., 2010. Treating viral exacerbations of chronic obstructive pulmonary disease: insights from a mouse model of cigarette smoke and H1N1 influenza infection. PLoS ONE 5, e13251.

Belisle, S.E., Tisoncik, J.R., Korth, M.J., Carter, V.S., Proll, S.C., Swayne, D.E., Pantin-Jackwood, M., Tumpey, T.M., Katze, M.G., 2010. Genomic profiling of tumor necrosis factor alpha (TNF-alpha) receptor and interleukin-1 receptor knockout mice reveals a link between TNF-alpha signaling and increased severity of 1918 pandemic influenza virus infection. J. Virol. 84, 12576–12588.

Borgeling, Y., Schmolke, M., Viemann, D., Nordhoff, C., Roth, J., Ludwig, S., 2014. Inhibition of p38 mitogen-activated protein kinase impairs influenza virus-induced primary and secondary host gene responses and protects mice from lethal H5N1 infection. J. Biol. Chem. 289, 13–27.

Brandes, M., Klauschen, F., Kuchen, S., Germain, R.N., 2013. A systems analysis identifies a feedforward inflammatory circuit leading to lethal influenza infection. Cell 154, 197–212.

Cameron, C.M., Cameron, M.J., Bermejo-Martin, J.F., Ran, L., Xu, L., Turner, P.V., Ran, R., Danesh, A., Fang, Y., Chan, P.K., Mytle, N., Sullivan, T.J., Collins, T.L., Johnson, M.G., Medina, J.C., Rowe, T., Kelvin, D.J., 2008. Gene expression analysis of host innate immune responses during Lethal H5N1 infection in ferrets. J. Virol. 82, 11308–11317.

Chakrabarty, K., Wu, W., Booth, J.L., Duggan, E.S., Nagle, N.N., Coggeshall, K.M., Metcalf, J.P., 2007. Human lung innate immune response to *Bacillus anthracis* spore infection. Infect. Immun. 75, 3729–3738.

Cloutier, A., Marois, I., Cloutier, D., Verreault, C., Cantin, A.M., Richter, M.V., 2012. The prostanoid 15-deoxy-Delta12,14-prostaglandin-j2 reduces lung inflammation and protects mice against lethal influenza infection. J. Infect. Dis. 205, 621–630.

Darwish, I., Mubareka, S., Liles, W.C., 2011. Immunomodulatory therapy for severe influenza. Expert Rev. Anti Infect. Ther. 9, 807–822.

de Jong, M.D., Simmons, C.P., Thanh, T.T., Hien, V.M., Smith, G.J., Chau, T.N., Hoang, D.M., Chau, N.V., Khanh, T.H., Dong, V.C., Qui, P.T., Cam, B.V., Ha do, Q., Guan, Y., Peiris, J.S., Chinh, N.T., Hien, T.T., Farrar, J., 2006. Fatal outcome of human influenza A (H5N1) is associated with high viral load and hypercytokinemia. Nat. Med. 12, 1203–1207.

Droebner, K., Pleschka, S., Ludwig, S., Planz, O., 2011. Antiviral activity of the MEK-inhibitor U0126 against pandemic H1N1v and highly pathogenic avian influenza virus in vitro and in vivo. Antiviral Res. 92, 195–203.

Fedson, D.S., 2013. Treating influenza with statins and other immunomodulatory agents. Antiviral Res. 99, 417–435.

Giulietti, A., Overbergh, L., Valckx, D., Decallonne, B., Bouillon, R., Mathieu, C., 2001. An overview of real-time quantitative PCR: applications to quantify cytokine gene expression. Methods 25, 386–401.

Ilyushina, N.A., Hay, A., Yilmaz, N., Boon, A.C., Webster, R.G., Govorkova, E.A., 2008. Oseltamivir-ribavirin combination therapy for highly pathogenic H5N1 influenza virus infection in mice. Antimicrob. Agents Chemother. 52, 3889–3897.

Iwasaki, A., Medzhitov, R., 2011. A new shield for a cytokine storm. Cell 146, 861–862.

Kandun, I.N., Tresnaningsih, E., Purba, W.H., Lee, V., Samaan, G., Harun, S., Soni, E., Septiawati, C., Setiawati, T., Sariwati, E., Wandra, T., 2008. Factors associated with case fatality of human H5N1 virus infections in Indonesia: a case series. Lancet 372, 744–749.

Kobasa, D., Jones, S.M., Shinya, K., Kash, J.C., Copps, J., Ebihara, H., Hatta, Y., Kim, J.H., Halfmann, P., Hatta, M., Feldmann, F., Alimonti, J.B., Fernando, L., Li, Y., Katze,

M.G., Feldmann, H., Kawaoka, Y., . Aberrant innate immune response in lethal infection of macaques with the 1918 influenza virus. Nature 445, 319–323.
Lauder, S.N., Jones, E., Smart, K., Bloom, A., Williams, A.S., Hindley, J.P., Ondondo, B., Taylor, P.R., Clement, M., Fielding, C., Godkin, A.J., Jones, S.A., Gallimore, A.M., 2013. Interleukin-6 limits influenza-induced inflammation and protects against fatal lung pathology. Eur. J. Immunol. 43, 2613–2625.
Liao, Q., Qian, Z., Liu, R., An, L., Chen, X., 2013. Germacrone inhibits early stages of influenza virus infection. Antiviral Res. 100, 578–588.
Ling, J.X., Wei, F., Li, N., Li, J.L., Chen, L.J., Liu, Y.Y., Luo, F., Xiong, H.R., Hou, W., Yang, Z.Q., 2012. Amelioration of influenza virus-induced reactive oxygen species formation by epigallocatechin gallate derived from green tea. Acta Pharmacol. Sin. 33, 1533–1541.
Londt, B.Z., Brookes, S.M., Nash, B.J., Nunez, A., Kelly, M.D., Garcon, F., Graham, S.P., Brown, I.H., 2013. Enhanced infectivity of H5N1 highly pathogenic avian influenza (HPAI) virus in pig ex vivo respiratory tract organ cultures following adaptation by in vitro passage. Virus Res. 178, 383–391.
Morin, J.P., Baste, J.M., Gay, A., Crochemore, C., Corbiere, C., Monteil, C., 2013. Precision cut lung slices as an efficient tool for in vitro lung physio-pharmacotoxicology studies. Xenobiotica 43, 63–72.
Nelli, R.K., Dunham, S.P., Kuchipudi, S.V., White, G.A., Baquero-Perez, B., Chang, P., Ghaemmaghami, A., Brookes, S.M., Brown, I.H., Chang, K.C., 2012. Mammalian innate resistance to highly pathogenic avian influenza H5N1 virus infection is mediated through reduced proinflammation and infectious virus release. J. Virol. 86, 9201–9210.
Pinto, R., Herold, S., Cakarova, L., Hoegner, K., Lohmeyer, J., Planz, O., Pleschka, S., 2011. Inhibition of influenza virus-induced NF-kappaB and Raf/MEK/ERK activation can reduce both virus titers and cytokine expression simultaneously in vitro and in vivo. Antiviral Res. 92, 45–56.
Punyadarsaniya, D., Liang, C.H., Winter, C., Petersen, H., Rautenschlein, S., Hennig-Pauka, I., Schwegmann-Wessels, C., Wu, C.Y., Wong, C.H., Herrler, G., 2011. Infection of differentiated porcine airway epithelial cells by influenza virus: differential susceptibility to infection by porcine and avian viruses. PLoS ONE 6, e28429.
Ranjith-Kumar, C.T., Lai, Y., Sarisky, R.T., Cheng Kao, C., 2010. Green tea catechin, epigallocatechin gallate, suppresses signaling by the dsRNA innate immune receptor RIG-I. PLoS ONE 5, e12878.
Reed, L.J., Muench, H., 1938. A simple method of estimating fifty per cent endpoints. Am. J. Epidemiol. 27, 493–497.
Sanderson, M.J., 2011. Exploring lung physiology in health and disease with lung slices. Pulm. Pharmacol. Ther. 24, 452–465.
Schroder, K., Hertzog, P.J., Ravasi, T., Hume, D.A., 2004. Interferon-gamma: an overview of signals, mechanisms and functions. J. Leukoc. Biol. 75, 163–189.
Seehase, S., Lauenstein, H.D., Schlumbohm, C., Switalla, S., Neuhaus, V., Forster, C., Fieguth, H.G., Pfennig, O., Fuchs, E., Kaup, F.J., Bleyer, M., Hohlfeld, J.M., Braun, A., Sewald, K., Knauf, S., 2012. LPS-induced lung inflammation in marmoset monkeys – an acute model for anti-inflammatory drug testing. PLoS ONE 7, e43709.
Siminski, J.T., Kavanagh, T.J., Chi, E., Raghu, G., 1992. Long-term maintenance of mature pulmonary parenchyma cultured in serum-free conditions. Am. J. Physiol. 262, L105–110.
Szretter, K.J., Gangappa, S., Lu, X., Smith, C., Shieh, W.J., Zaki, S.R., Sambhara, S., Tumpey, T.M., Katz, J.M., 2007. Role of host cytokine responses in the pathogenesis of avian H5N1 influenza viruses in mice. J. Virol. 81, 2736–2744.
Van Poucke, S.G., Nicholls, J.M., Nauwynck, H.J., Van Reeth, K., 2010. Replication of avian, human and swine influenza viruses in porcine respiratory explants and association with sialic acid distribution. Virol. J. 7, 38.
Wang, W., Yang, P., Zhong, Y., Zhao, Z., Xing, L., Zhao, Y., Zou, Z., Zhang, Y., Li, C., Li, T., Wang, C., Wang, Z., Yu, X., Cao, B., Gao, X., Penninger, J.M., Wang, X., Jiang, C., 2013. Monoclonal antibody against CXCL-10/IP-10 ameliorates influenza A (H1N1) virus induced acute lung injury. Cell Res. 23, 577–580.
Weiss, I.D., Wald, O., Wald, H., Beider, K., Abraham, M., Galun, E., Nagler, A., Peled, A., 2010. IFN-gamma treatment at early stages of influenza virus infection protects mice from death in a NK cell-dependent manner. J. Interferon Cytokine Res. 30, 439–449.
Wu, W., Booth, J.L., Duggan, E.S., Wu, S., Patel, K.B., Coggeshall, K.M., Metcalf, J.P., 2010. Innate immune response to H3N2 and H1N1 influenza virus infection in a human lung organ culture model. Virology 396, 178–188.
Zarogiannis, S.G., Noah, J.W., Jurkuvenaite, A., Steele, C., Matalon, S., Noah, D.L., 2012. Comparison of ribavirin and oseltamivir in reducing mortality and lung injury in mice infected with mouse adapted A/California/04/2009 (H1N1). Life Sci. 90, 440–445.
Zhang, J.H., Chung, T.D., Oldenburg, K.R., 1999. A simple statistical parameter for use in evaluation and validation of high throughput screening assays. J. Biomol. Screen. 4, 67–73.